Am J Transl Res 2017;9(9):3935-3949
www.ajtr.org /ISSN:1943-8141/AJTR0051348

Original Article

Reduced beta 2 glycoprotein I prevents high glucose-induced cell death in HUVECs through miR-21/PTEN

Jing-Yun Zhang*, Jun Ma*, Pei Yu, Guang-Jie Tang, Chun-Jun Li, De-Min Yu, Qiu-Mei Zhang

*Key Laboratory of Hormones and Development (Ministry of Health), Tianjin Key Laboratory of Metabolic Diseases, Tianjin Metabolic Diseases Hospital & Tianjin Institute of Endocrinology, Tianjin Medical University, 300070 Tianjin, China. *Equal contribution.*

Received February 21, 2017; Accepted August 13, 2017; Epub September 15, 2017; Published September 30, 2017

Abstract: High serum beta 2 glycoprotein I (β2GPI) is associated with complications of type 2 diabetes mellitus (DM), and especially microvascular disorders. In contrast, reduced β2GPI (Rβ2GPI) can prevent diabetic vascular injury. This study aimed to investigate the protective function of Rβ2GPI in DM vascular disorders, and to assess the under lying mechanisms. High glucose-induced injury in human umbilical vein endothelial cells (HUVECs) was used to model hyperglycemia. Alow concentration of Rβ2GPI (0.5 μM), but not β2GPI, mitigated high glucose-induced cell injury. High glucose decreased miR-21 expression and Akt phosphorylation at 6 h, but facilitated their expression at 48 h. Moreover, high glucose decreased phosphatase and tensin homolog deleted on chromosome ten(PTEN) expression at 6 h, but facilitatedits expression at 48 h. Importantly, by promoting miR-21 expression, Rβ2GPI mitigated high glucose-induced PTEN expression, reduced Akt phosphorylation and nitric oxide synthase activity, and increased cyclooxygenase-2 activity and cell loss. Similar to Rβ2GPI, an miR-21 mimic (1 pM) and PTEN inhibition (1 μM bpV, or PTEN silencing) exerted protective action, while an Akt signaling pathway inhibitor (LY294002, 1 μM) aborted the effect of Rβ2GPI on high glucose-induced cell injury. Finally, Rβ2GPI inhibited high glucose-induced apoptosis via a mitochondria-dependent pathway. These data reveal that Rβ2GPI exerts protective action in high glucose-induced HUVEC injury. The mechanism is related to the miR-21-PTEN-Akt pathway and mitochondria-dependent apoptosis. This study provides *in vitro* data supporting the therapeutic effect of Rβ2GPI in diabetic vascular injury.

Keywords: Reduced beta 2 glycoprotein I, HUVECs, miR-21, PTEN, nitric oxide

Introduction

Diabetes mellitus (DM) affects approximately 100 million people worldwide and the incidence is increasing as a consequence of lifestyle patterns contributing to obesity [1]. As vascular diseases are the principal cause of death and disability in DM patients, vascular complications of DM are now attracting increased attention [2]. Although the mechanisms underlying vascular disorders in DM are not completely understood, hyperglycemia is the most consistent and significant factor correlated with vascular disorders in DM [3]. Vascular endothelial cell dysfunction has been widely reported in DM animals [4-6]. Therefore, a lot of investigations are now focusing on finding effective approaches to prevent hyperglycemia-induced endothelial cell injury [7-9].

Beta 2 glycoprotein I (β2GPI) is predominantly synthesized in hepatocytes [10] and hasnow been identified as the most prominent antigen in antiphospholipid syndrome [11, 12]. Structurally, β2GPI consists of five repeating amino acid domains. Domains I-IV include four cysteinesand have conserved sequences and domain V has an extra 20 amino acid tail with a unique cysteine termination [13]. The current research group previously reported that domain I-IV of β2GPI inhibited advanced glycation end product-induced angiogenesis by down-regulating vascular endothelial growth factor 2 signaling [14]. Intriguingly, it has been demonstrated that the disulfide bond between Cys288 to Cys326 in the domain V can be reduced by thioredoxin-1 (TRX-1) or protein disulfide isomerase [15], resulting in the reduced state of β2GPI (Rβ2GPI). β2GPI is a participant in the immune system, vascular thrombosis, infectious diseaseand other systems [16-18]. β2GPI is also associated with accelerated atherosclerosis and enhanced oxidative stress [19]. In addition,

high serum β2GPI is associated with complications of type 2 DM [20], especially diabetic microvascular complications [21]. In contrast, Rβ2GPI has been found to protect endothelial cells from oxidative stress-induced injury [19]. The current research group has also demonstrated that Rβ2GPI inhibited vascular endothelial growth factor and basic fibroblast growth factor-induced angiogenesis [22] and the redox status of β2GPI was found to be important in different stages of diabetic angiopathy [23]. Therefore, it is of interest to determine the effects of Rβ2GPI in diabetic microvascular complications and the underlying mechanisms.

Phosphatase and tensin homolog deleted on chromosome ten (PTEN) contains a tensin-like domain as well as a catalytic domain similar to that of the dual specificity protein tyrosine phosphatases. This protein was first identified as a tumor suppressorand negatively regulates intracellular levels of phosphatidylinositol-3, 4,5-trisphosphate in cells and functions as a tumor suppressor by negatively regulating theprotein kinase B (Akt) signaling pathway [24]. In a previous study, PTEN wasreported to be upregulated after high glucose treatment in endothelial cells, which implied that PTEN could be a potential target for the treatment of high glucose-induced cell injury [8]. However, the mechanism underlying high glucose-induced PTEN expression is still elusive. The current study aimed to investigate the effect of Rβ2GPI on hyperglycemia-induced endothelial cell injury, and to assess the under lying mechanisms. The study provides important evidence for the protective action of Rβ2GPI in vascular complications of DM.

Material and methods

Reagents

PTEN inhibitor [bpV (phen)] (CAS 42494-73-5, EMD Chemicals, Inc, Gibbstown, NJ, USA); miR-21 mimic (Guangzhou Ruibo, Guangzhou, China);3-(4,5-Dimethylthiazol-2-Yl)-2,5-Diphenyltetrazolium Bromide (Gibco, USA); Glucose (Sigma, USA); PTEN-small interfering RNA (siRNA) (#6251) and normal control (NC)-siRNA were obtained from CST (USA).

Cell culture and groups

All the protocols were approved by the Ethical Committee of Tianjin Medical University Metabolic Disease Hospital (Ethics protocol number: DXBYYhMEC2017-11). Endothelial cells from human umbilical cord veins (HUVECs) were harvested as previously described [25]. In brief, human umbilical cord tissue was digested using 0.05% collagenasefor 15 min at 37°C. The cells were filtered andsuspended in M199 medium including fetal calf serum (20%) and incubated in a humidified atmosphere with 5% CO_2 at 37°C. Culture medium was refreshed every 2 days and adherent cells were identified by their cobblestone appearance at confluence and positive labelling with mouse fluorescein isothiocyanate-conjugated antihuman factor VIII. Cells in theirsecond passage wereused in the experiments.

As the physiological concentration of Rβ2GPI is approximately 4 μM, a safe concentration of Rβ2GPI was determined in the *in vitro* cultured HUVECs using an 3-(4,5-dimethyl-2-thiazolyl)-2,5-diphenyl-2h-tetrazolium bromide (MTT) assay. After that, a relatively high concentration of Rβ2GPI, which did not demonstrate cytotoxic action (0.5 μM), was selected to investigate the protective effect of Rβ2GPI in high glucose-induced cell injury. The cell samples were divided into a control group (normal glucose), a model group (high glucose), a 0.5 μM Rβ2GPI treatment group (high glucose [HG]+Rβ2GPI), a 0.5 μM β2GPI treatment group (HG+β2GPI), a 0.5 μM Rβ2GPI control group (Rβ2GPI) and a vehicle treatment group (HG+TRX-1, dithiothreitol [DTT] and glutathione). The high glucose-induced cytotoxicity model in HUVECs was performed as previously described [7]. Cells in the control group were treated with normal levels of glucose (5.5 mM), while in the high glucose group the cells were treated with a high concentration of glucose (44.4 mM). To keep the cells in quiescence, the concentration of fetal bovine serum in the culture medium was reduced to 2% in all groups treated using high glucose. In some of the experiments, a miR-21 mimic, PTEN-siRNA, a PTEN inhibitor and an Akt inhibitor were employed to study the mechanisms involved. There were six replicates in each group in each experiment.

Purification of β2GPI and preparation of Rβ2GPI

β2GPI was purified from normal human plasma as previously described [26] and Rβ2GPI was

prepared following amethod detailed in a previous publication [27]. In brief, purified β2GPI (2 μM) was reduced using TRX-1 (3.5 μM) activated with DTT (70 μM). The thiols of Rβ2GPI were protected by reduced glutathione. Rβ2GPI levels and structure were confirmed as previously described [19, 28, 29].

Cell viability

HUVECs were seeded in 96-well plates and cultured for 5 days. The cells were incubated with different concentrations of Rβ2GPI (0.25-1 μM). Aftera 48 h incubation, cell viability was detected using an MTT assay. In other experiments, the protection of Rβ2GPI in high glucose-induced cell injury was assessed. After the indicated drug treatment, 20 μL of MTT (5 mg/mL) was added into the 180 μL culture medium in each well. The medium was removed aftera 4 h incubation, and 150 μL of dimethyl sulphoxide was added into each well to dissolve the precipitate. The absorbance was measured at a wavelength of 490 nm using an automated microplate reader (Multiskan FC, Thermo Scientific, USA). Cell viability was calculated using the following formula: cell viability (%) = average absorbance of each group/average absorbance of control group × 100%.

SmaII interfering RNA

RNA interference-mediated knockdown of PTEN was performed through transfection of synthetic duplex RNA oligonucleotides, using Oligofectamine (Invitrogen, Carlsbad, CA, USA) according to the manufacturers' instructions. PTEN-siRNA and scrambled siRNA were used in the current study and the protocol was performed as previously described [30]. Cells were grown in 90 mm dishes and were transfected at 70% confluence. The medium was changed after 6 h and high glucose was added to the cells. After 48 h of culturing, protein expression and cell viability were assessed.

Detection of intracellular free Ca^{2+}

Intracellular free Ca^{2+} levels were assessed using fluo 3-acetoxymethyl (AM) (Beyotime Biotechnology, China) following the instructionsprovided with the kit. HUVECs were seeded in 96-well plates. After various treatments for 48 h, the cells were washed using phosphate-buffered saline (PBS) and incubated in serum-free medium containing 5 μM flura-3/AM for 60 min at 37°C. After that, the cells were washed using PBS and cultured for another 25 min to ensure conversion of fluro-3/AM into fluro-3. The excitation and emission wavelengths were set at 488 and 530 nm respectively, to measure the fluro-3 fluorescence.

Determination of total nitric oxide (NO), nitic oxide synthase (NOS) and cyclooxygenase-2 (COX-2) activity

HUVECs were seeded in 12-well plates. After various treatments, the culture medium was collected to measure the NO levelusing an NO assay kit (Nanjing Jiancheng Bioengineering Institute, China). Briefly, 2×10^6 cells were collected after trypsin digestion and washed using cold PBS. The cells were resuspended in 100 μL of ice cold Assay Buffer and homogenized quickly by pipetting up and down a few times. The samples were centrifuged for 2-5 min at 4°C at top speed (12000 × g). The supernatant was collected and transferred to a clean tube. Ice cold perchloric acid (PCA) (4 M) was added to achieve a final concentration of 1 M in the homogenate solution which was vortexed briefly to mix it well. After the deproteinization step, the supernatant was collected for absorbance detection. The absorbancewas detected using a spectrophotometer at 540 nm. The NO level was calculated as follows: NO (μM) = [(absorbance of treated wells-absorbance of blank wells)/(absorbance of standard wells-absorbance of blank wells) × standard concentration (100 μM)].

NOS activity was detected by following the instructionsprovided with the kit (Beyotime, Ningbo, China). After various treatments, the cells were collected to measure the NOS activity, as previously described [31]. Briefly, 2×10^6 cells were collected after trypsin digestion and washed using cold PBS. The cells were resuspended in 100 μL of ice cold Assay Buffer and homogenized quickly by pipetting up and down a few times. The samples were centrifuged for 2-5 minutes at 4°C at top speed (12000 × g). The supernatant was collected and transferred to a clean tube. A fluorimeter was used, with an excitation wavelength of 490 nm and an emission wavelength of 520 nm. After preparation of the appropriate reaction mixtures, the assay was carried out in a 96-well plate. A total of

200 μL of reaction mixture was added into each well and incubated for 2 h at room temperature in the dark.

COX-2 activity was measured by following the instructions provided with the kit (ab210574, Abcam, USA). After various treatments, the cells were collected and underwent lysis. All samples were performed in duplicate and were allowed to warm to room temperature and all activity measurements were performed at room temperature. A total of 50 μL of tris-phenol buffer, 50 μL of hematin solution and 50 μL of the sample were added to each well. After pre-incubation at room temperature for 5 min, 25 μL of nonsteroidal anti-inflammatory drugs (NSAIDs) inhibitor solution was added to the appropriate wells and incubated at room temperature for 5-120 minutes (dependent on the inhibitor). The microtiter plate was placed in aluminometer for the chemiluminescence measurement. A total of 50 μL of cold COX Chemiluminescent Substrate and 50 μL of diluted cold arachidonic acid solution wereadded to each well and the samples were measured in a luminometer for 5 s. The relative light units were calculated.

Immunoblot analysis

Cytoplasmic protein was isolated using a Cytoplasmic Protein Extraction kit (Beyotime, Jiangsu, China). The cells were treatedusing the indicated drugs, washed with 1 mL of ice-cold PBS, and collected and centrifuged for 5 min at 1150 × g at 4°C. Protein concentration was measured using the bicinchoninic acid method (Beyotime, China), and an equal amount of protein (20 μg) was loaded into 10% sodium dodecyl sulfate-polyacrylamide gel electrophoresis gels. The membranes were incubated with anti-PTEN (Ser-2448, 1:1000; #9559, CST, USA), anti-Akt (1:1000; #4685, CST, USA), anti-phospho-Akt (1:1000; #9271, CST, USA), anti-Bcl-2 (1:1000; #4223, CST, USA), anti-Bax (1:1000; #2774, CST, USA) and anti-Actin (1:5000; #3700, CST, USA) at 4°C overnight. After washing, the membranes were incubated with a secondary antibody (1:5000; CST, USA). The signal was detected using an enhanced chemiluminescence detection kit (Amersham ECL RPN 2106 Kit, Amersham Pharmacia Biotech, QC, Canada).

Real-time PCR

Total RNA was extracted according to the instruction sprovided with the Trizol kit (Dalian Baosheng, Dalian, China) and the purity of the RNA was confirmed using optical density measurements (280/260). RNA was amplified using a one-step real-time (RT)-PCR kit (Dalian Baosheng, Dalian, China). The primers were added into a 25-μL PCR reaction system following a protocol of 94°C denaturation for 45 s, 59°C annealing for 45 s, and 72°C extension for 60 s, for 35 cycles. The primers are listed as follows (5'-3'): miR-21-F: ACACTCCAGCTGGGTAGCTTAT, miR-21-R: TGGTGTCGTGGAGTCG; U6-F: CTGCTTCGGCAGCACA, U6-R: AACGCTTCACGAATTTGCGT; PTEN-F: CCAAGCTTATGACAGCCATCATC, PTEN-R: CGCGGATCCTCAGACTTTTGTAA; β-actin-F: GAATCAATGCAAGTTCGGTTCC, β-actin-R: TCATCTCCGCTATTAGCTCCG. All the mRNA expression levels were calculated based on the comparative quantification method ($2^{-\Delta\Delta CT}$), as previously described [32]. U6 and β-actin were used as internal controls for miR-21 (ID: 100314000) and PTEN (ID: 19211) mRNA quantitation, respectively.

Relative luciferase activity

A miR-21 mimic (5'-UAGCUUAUCAGACUGAUGUUUA3'), and the plasmids Mut PTEN 3'-UTR (5'-UAGUCAUCACUGUAUUAGGGUA-3') and WT PTEN 3'-UTR (5'-UAGUCAUCACUGUAAUAAGUU-3'), were transfected into HUVECs using Lipofectamine™ 2000, in accordance with the provided instructions. Plasmids encoding an effective sequence to knock down the expression of PTEN and the NC-siRNA sequence were constructed. A dual luciferase detection system was applied to detect luciferase activity. After transfection for 24 h, the medium was removed, and the cells were washed using PBS and 100 μL of passive lysis buffer was added and the samples were incubated for 10 min. Following centrifugation (11150 × g) for 10 min, the supernatant was collected. A total of 20 μL of supernatant and 100 μL of luciferase assay reagent were mixed. Firefly luciferase activity was determined using a Glomax 20/20 fluorescence luminometer. After that, 100 μL of Stop&Glo reagent was added to detect Renilla luciferase activity. The relative fluorescence was calculated.

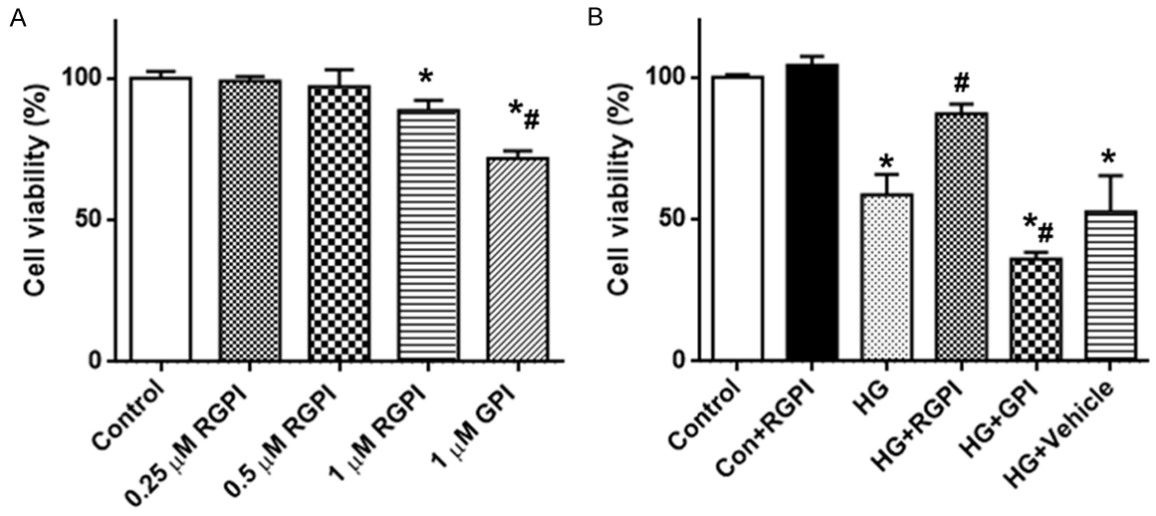

Figure 1. Reduced β2GPI prevents high glucose-induced decrease of cell viability. A. The effects of reduced or non-reduced β2GPI on the cell survival in HUVECs. Data were presented as means and SEM. Six replications were carried out in each group. *P<0.05 compared with control. #P<0.05 compared with 1 μM reduced β2GPI; B. The effects of reduced or non-reduced β2GPI on high glucose-induced cell death in HUVECs. Data were presented as means and SEM. Six replications were carried out in each group. *P<0.05 compared with control; #P<0.05 compared with high glucose (HG).

Caspase activity assay

Caspase-3 and caspase-9 activities were detected in accordance with the instructions provided with the assay kits (Cloud Clone, Houston, Texas, USA), and as previously described [33].

Statistical analysis

The data are presented as means ± standard error of mean. Statistical analyses of the data were performed using Graphpad software. When only two groups were compared, a two-tailed t-test was used to determine statistical significance. When more than two groups were compared, a one-way or two-way analysis of variance (ANOVA) was selected followed by a Bonferroni post hoc test to determine statistical significance. *P* values of less than 0.05 are considered statistically significant.

Results

Rβ2GPI attenuates high glucose-induced cell death in HUVECs

Initially, the cell viability of HUVECs aftertreatment with Rβ2GPI for 48 h was assessed. Rβ2GPI at concentrations of 0.25 μM and 0.5 μM did not affect thecell viability of HUVECs after a 48 h treatment (**Figure 1A**). However, a 1 μM Rβ2GPI treatment for 48 h significantly decreased the cell viability to 85% of control, while β2GPI (1 μM) further decreased the cell viability to 70% of control (P=0.02 vs control, P=0.012 vs 1 μM Rβ2GPI). However, 0.5 μM Rβ2GPI did not have cytotoxic action in HUVECs after a 48 h treatment. In the following experiments, 0.5 μM Rβ2GPI was selected to investigate the effects of Rβ2GPI on high glucose-induced cell injury in HUVECs, and to assess the underlying mechanisms.

As shown in **Figure 1B**, after a 44.4 mM glucose treatment for 48 h, the cell viability decreased to 50%, whereas a 0.5 μM Rβ2GPI co-application significantly mitigated high glucose-induced cell injury (cell viability: 85%; P=0.02 vs control). In contrast, non-reduced β2GPI further decreased the cell viability compared with the high glucose group (P=0.03). However, the vehicle (TRX-1, DTT and glutathione) did not exert protective action against the high glucose-induced cell death (P=0.5). These results suggest that 0.5 μM Rβ2GPI was beneficial for cell survival in a high glucose-inducedcell injury model.

Rβ2GPI reverses the high glucose-induced increase in PTEN

Previous reports have revealed that high glucose promotes PTEN expression in HUVECs aftera 48 h treatment [8]. In the current study, a time-dependent effect of high glucose on

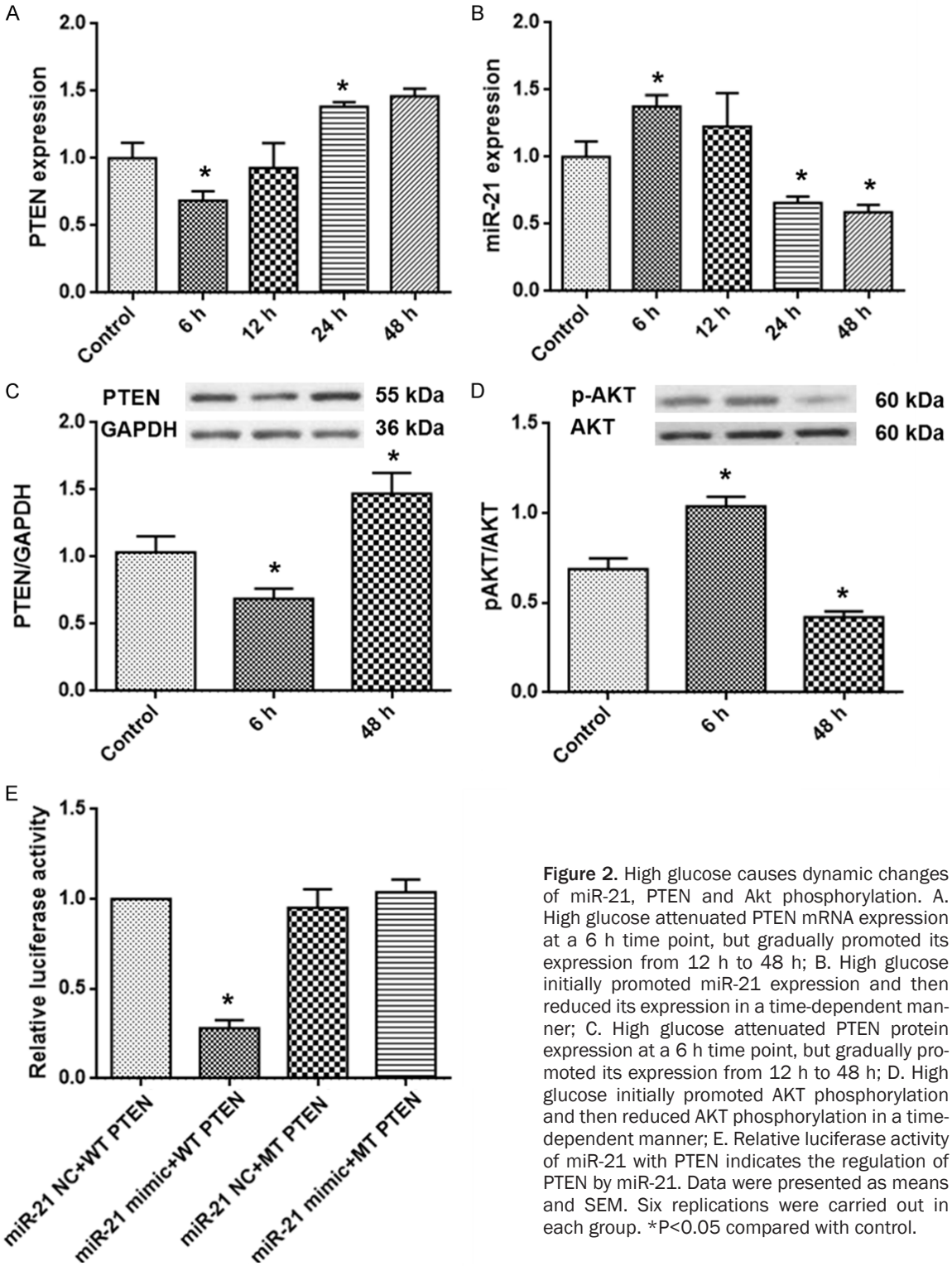

Figure 2. High glucose causes dynamic changes of miR-21, PTEN and Akt phosphorylation. A. High glucose attenuated PTEN mRNA expression at a 6 h time point, but gradually promoted its expression from 12 h to 48 h; B. High glucose initially promoted miR-21 expression and then reduced its expression in a time-dependent manner; C. High glucose attenuated PTEN protein expression at a 6 h time point, but gradually promoted its expression from 12 h to 48 h; D. High glucose initially promoted AKT phosphorylation and then reduced AKT phosphorylation in a time-dependent manner; E. Relative luciferase activity of miR-21 with PTEN indicates the regulation of PTEN by miR-21. Data were presented as means and SEM. Six replications were carried out in each group. *P<0.05 compared with control.

PTEN expression was detected using real-time PCR. As shown in **Figure 2A**, high glucose attenuated PTEN expression at a 6 h time point, but gradually promoted its expression from 12 h to 48 h. It has been demonstrated that PTEN expression is regulated by miR-21 [34]. In the current study, increased miR-21 expression was observed after high glucose

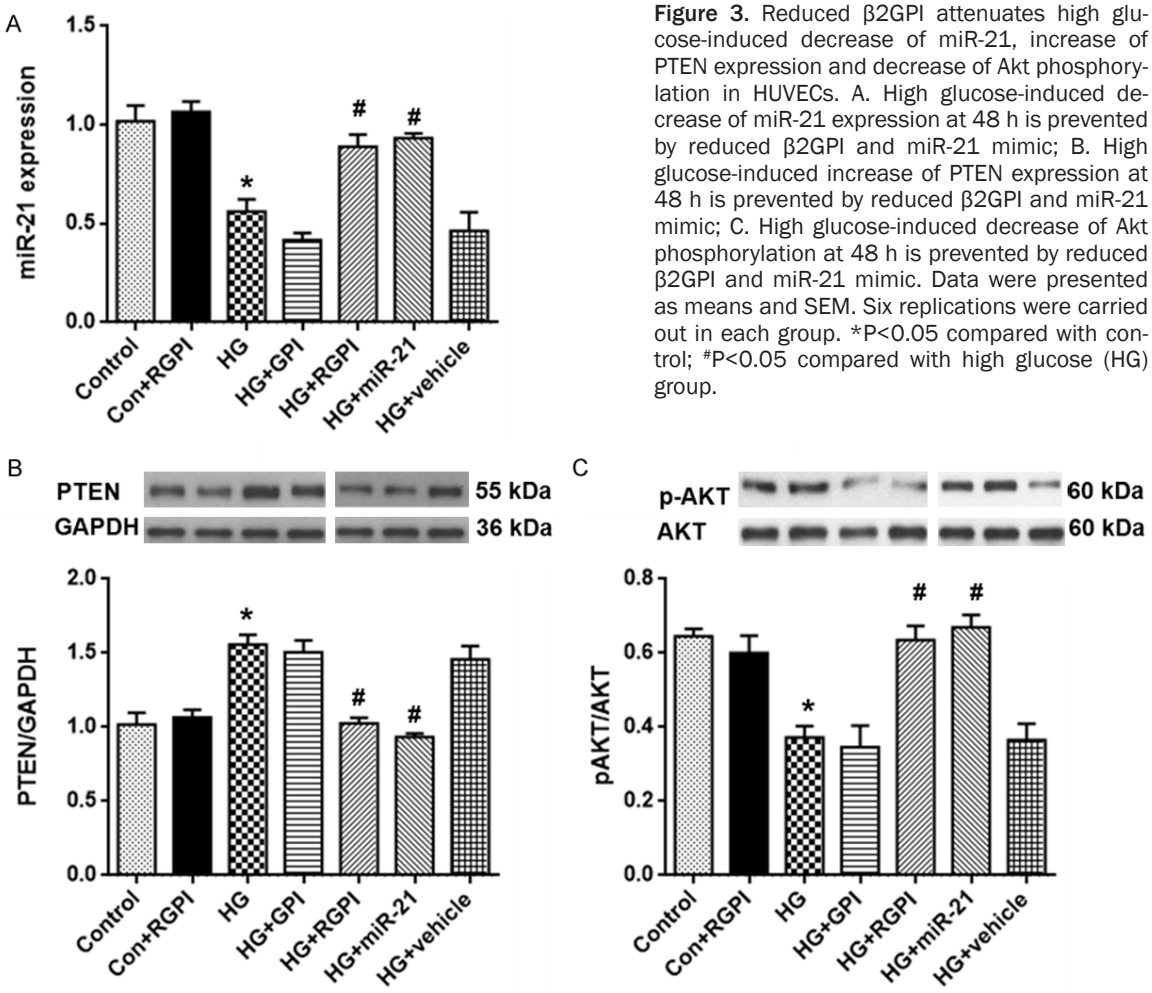

Figure 3. Reduced β2GPI attenuates high glucose-induced decrease of miR-21, increase of PTEN expression and decrease of Akt phosphorylation in HUVECs. A. High glucose-induced decrease of miR-21 expression at 48 h is prevented by reduced β2GPI and miR-21 mimic; B. High glucose-induced increase of PTEN expression at 48 h is prevented by reduced β2GPI and miR-21 mimic; C. High glucose-induced decrease of Akt phosphorylation at 48 h is prevented by reduced β2GPI and miR-21 mimic. Data were presented as means and SEM. Six replications were carried out in each group. *P<0.05 compared with control; #P<0.05 compared with high glucose (HG) group.

treatment. As shown in **Figure 2B**, high glucose triggered miR-21 expression, which was inversely correlated with the effect of high glucose on PTEN expression. High glucose initially promoted miR-21 expression and then reduced its expression in a time-dependent manner. PTEN expression was assessed at the protein level at 6 h and 48 h time points. Consistent with the mRNA expression, high glucose also reduced PTEN protein expression at 6 h and up-regulated its expression 48 h after treatment (**Figure 2C**). As PTEN is a negative regulator of the Akt signaling pathway [35], Akt phosphorylation after high glucose treatment was assessed. As shown in **Figure 2D**, high glucose promoted Akt phosphorylation at the 6 h time point, but reduced Akt phosphorylation at the 48 h time point. To assess the direct regulation of PTEN by miR-21, a luciferase reporter assay was performed. As shown in **Figure 2E**, a miR-21 mimic significantly decreased the relative fluorescence in the group transfected using wild type PTEN 3'UTR. These data suggest that high glucose inversely regulates PTEN and Akt phosphorylation in the acute phase and in chronic phases.

The 48 h time point was selected for further experiments after the indicated drug treatments. As shown in **Figure 3A**, miR-21 expression in the high glucose group was significantly reduced compared with the control (P=0.001). The decrease was mitigated by Rβ2GPI (vs the model group; P=0.01), but not by β2GPI. A miR-21 mimic (1 pM) was also designed to test whether exogenous supplemental miR-21 could reverse the detrimental effects of high glucose. As predicted, the miR-21 mimicreversed the high glucose-induced decrease in miR-21 levels (vs the model group; P=0.02).

PTEN expression after Rβ2GPI treatment in the high glucose-induced cell injury model was also tested. As shown in **Figure 3B**, high glucose

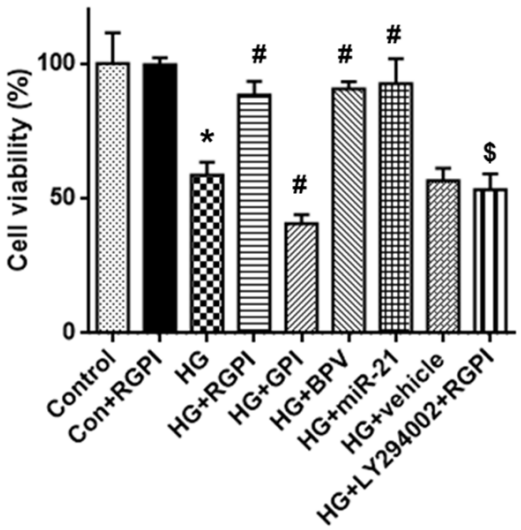

Figure 4. Reduced β2GPI attenuates high glucose-induced cell death in HUVECs via regulating miR-21-PTEN. miR-21 mimic and bpV ameliorated high glucose-induced cell injury. AKT inhibitor prevents the protection of reduced β2GPI. Data were presented as means and SEM. Six replications were carried out in each group. *P<0.05 compared with control; #P<0.05 compared with high glucose (HG) group; $P<0.05 compared with high glucose (HG)+RGPI group.

promoted PTEN expression (vs control; P=0.02), which was eliminated by Rβ2GPI treatment (vs the model group; P=0.02), but not by β2GPI. Importantly, the miR-21 mimic also mitigated high glucose-induced PTEN expression (vs the model group; P=0.04). Akt phosphorylation was also examined in the different groups. As shown in **Figure 3C**, high glucose depressed Akt phosphorylation (vs control; P=0.01), which was facilitated by Rβ2GPI treatment (vs the model group; P=0.02), but not by β2GPI. The miR-21 mimic also promoted the high glucose-induced decrease of Akt phosphorylation (vs the model group; P=0.01). These data suggest that Rβ2GPI exerted protection in high glucose-induced cell injury in HUVECs likely through miR-21 and PTEN.

Rβ2GPI attenuates high glucose-induced cell deathvia regulation of the miR-21-PTEN-Akt pathway

Rβ2GPI reversed high glucose regulation of the miR-21-PTEN-Akt signaling pathway in HUVECs, and the current study aimed to determine whether this signaling pathway was responsible for the protection of Rβ2GPI in high glucose-induced cell injury. Therefore, cell viability was assessed in different conditions. As shown in **Figure 4**, high glucose decreased cell viability in HUVECs compared with control (P=0.02), which was reversed by Rβ2GPI treatment (vs the model group; P=0.02), but not by β2GPI. A miR-21 mimicameliorated high glucose-induced cell injury (vs the model group; P=0.02). Interestingly, 1 μM bpV also ameliorated high glucose-induced cell injury (vs the model group; P=0.03). Additionally, the LY294002 phosphoinositide 3-kinaseinhibitor (1 μM) blocked the protective effect of Rβ2GPI (vs HG+Rβ2GPI; P=0.01).

Another set of experiments were carried out to knock down PTEN expression. Compared with high glucose treatment alone, PTEN-siRNA significantly reduced PTEN expression (P=0.02; **Figure 5A**), promoted Akt phosphorylation (P=0.03; **Figure 5B**) and prevented high glucose-induced cell injury (P=0.03; **Figure 5C**). In contrast, NC-siRNA did not alter PTEN and p-Akt expression, and high glucose-induced cell death (**Figure 5**).

Rβ2GPI reverses high glucose-induced intracellular free Ca^{2+} levels

The intracellular free Ca^{2+} levels in the different groups were examined. As shown in **Figure 6**, high glucose increased intracellular calcium levels compared with the control (P=0.02), which was reversed by Rβ2GPI treatment (vs the model group; P=0.04) but not by β2GPI. The miR-21 mimic also eliminated the high glucose-induced increase in intracellular free Ca^{2+} levels (vs the model group; P=0.02). Interestingly, the bpV PTEN inhibitor also eliminated the high glucose-induced increase in intracellular free Ca^{2+} levels (vs the model group; P=0.03).

Rβ2GPI reverses the high glucose-induced decrease in NO production and NOS activity

NO production and NOS activity were also measured. As shown in **Figure 7A**, high glucose decreased NO production compared with control, which was reversed by Rβ2GPI treatment (vs the model group; P=0.03), but not by β2GPI. The miR-21 mimicpromoted the high glucose-induced decrease in NO production. Interestingly, a PTEN inhibit oral so promoted the high glucose-induced decrease in NO production.

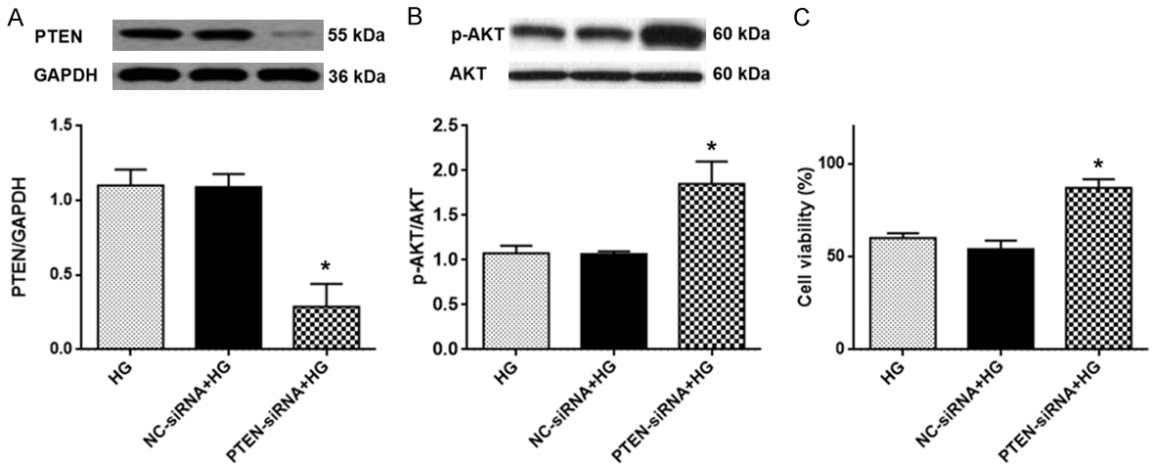

Figure 5. PTEN-siRNA reduces PTEN expression, promotes Akt phosphorylation and prevented cell death in high glucose-induced HUVECs. A. PTEN expression; B. Akt and p-Akt expression; C. Cell viability. Data were presented as means and SEM. Six replications were carried out in each group. *P<0.05 compared with NC-siRNA+high glucose (HG).

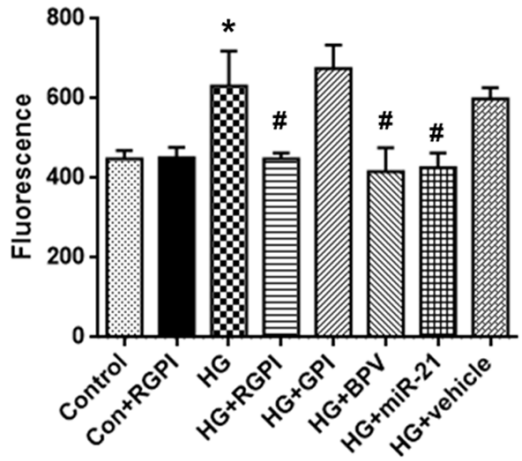

Figure 6. Reduced β2GPI prevents high glucose-induced intracellular free calcium levels in HUVECs. The cells were incubated with reduced or non-reduced β2GPI for 48 h. After that, the intracellular free calcium level was tested. Data were presented as means and SEM. Six replications were carried out in each group. *P<0.05 compared with control; #P<0.05 compared with HG group.

NOS is required for NO production [36]. Experiments were also conducted to detect NOS activity in the different groups. As shown in **Figure 7B**, high glucose decreased NOS activity compared with control, which was ameliorated by Rβ2GPI but not by β2GPI (vs the model group; P=0.035). The miR-21 mimic, as well as bpV, promoted the high glucose-induced decrease in NOS activity.

Rβ2GPI reverses the high glucose-induced increase in COX-2 activity

COX-2 activity after Rβ2GPI treatment was also assessed. As shown in **Figure 8**, high glucose increased COX-2 activity compared with control, which was reversed by Rβ2GPI treatment (vs the model group; P=0.03) but not by β2GPI. The miR-21 mimic, as well as bpV, promoted the high glucose-induced increase in COX-2 activity.

Rβ2GPI reverses high glucose-induced apoptosis

High glucose elicited cell death, mainly through inducing apoptosis in the HUVECs [7]. Caspase 3 and caspase 9 activities were assessed to investigate this effect. As shown in **Figure 9A** and **9B**, high glucose increased caspase 3 and caspase 9 activity compared with control, which was reversed by Rβ2GPI treatment but not by β2GPI. A miR-21 mimic, as well as bpV, reversed the high glucose-induced increase in caspase activity. Additionally, it was observed that high glucose promoted Bax expression and decreased Bcl-2 expression, which were ameliorated by Rβ2GPI treatment (**Figure 9C**).

Discussion

Although β2GPI is a participant in antiphospholipid syndrome, as well as in DM, thecurrent study has demonstrated the potential mechanisms underlying the protective action of

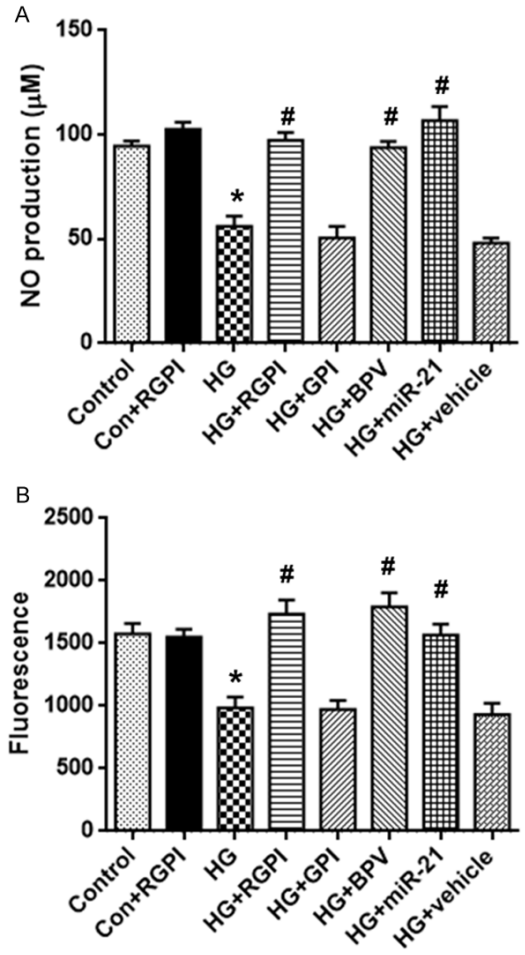

Figure 7. Reduced β2GPI prevents high glucose-induced decrease of NO production in HUVECs. The cells were incubated with reduced and high glucose for 48 h. After that, the NO level and NOS activity were tested. A. NO level. B. NOS activity. Data were presented as means and SEM. Six replications were carried out in each group. *P<0.05 compared with control; #P<0.05 compared with HG group.

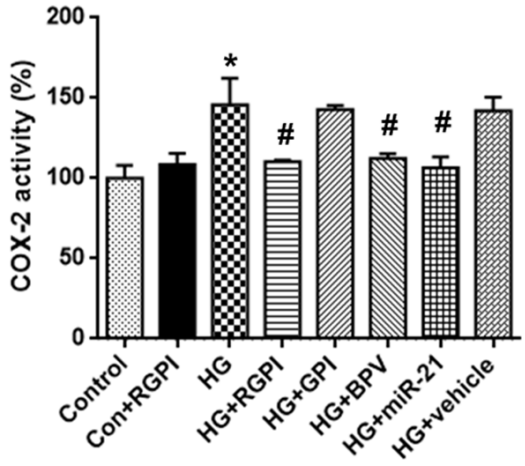

Figure 8. Reduced β2GPI prevents high glucose-induced increase of COX-2 activity in HUVECs. The cells were incubated with reduced or non-reduced β2GPI for 48 h. After that, the COX-2 activity was tested. Data were presented as means and SEM. Six replications were carried out in each group. *P<0.05 compared with control; #P<0.05 compared with HG group.

Rβ2GPI in the vascular complications of DM. *In vitro* experiments showed that Rβ2GPI exerted protection against high glucose-induced cell injury. Importantly, miR-21-PTEN-Akt was implicated as the potential target involved in the protection.

As previously reported, the proportion of Rβ2GPI is decreased in antiphospholipid syndrome [37, 38]. Although there were no definite evidence showing that β2GPI reduction could fight against the disease progression, Rβ2GPI, rather than non-Rβ2GPI, was reported to protect human umbilical vein cell linefrom oxidative stress-induced endothelial cell damage [29]. In thecurrent study, a protective action of Rβ2GPI in high glucose-induced endothelial cell injury was identified. High glucose levels, as well as the related increasein osmotic pressure, impair the function of endothelial cells. High glucose increased the osmotic pressure from 312 Osmol/L in normal culture medium, to 450 Osmol/L. Therefore, high glucose is widely applied to model the *in vitro* damage of endothelial cells as encountered in DM. In the current study, it was observed that Rβ2GPI at the concentrations of 0.25 μM and 0.5 μM did not affect cell viability after a 48 h treatment, which indicated that this dose range of Rβ2GPI was safe for endothelial cells. However, 1 μM Rβ2GPI decreased the cell viability. The toxicity might be caused by the re-oxidation of β2GPI, as non-Rβ2GPI was also detrimental to HUVECs. In contrast with a previous publication, which showed thatboth β2GPI and Rβ2GPI improved kidney fibrosis [28], the current study found that only Rβ2GPI exerted protection in high glucose-induced cell injury in HUVECs. The osmotic pressure in the medium of the Rβ2GPI and high glucose co-treatment group was not significantly different from that of the high glucose group, which suggests that Rβ2GPI did not regulate the osmotic pressure to exert protection.

PTEN was first reported as a tumor suppressor [24]. Accumulating evidence also suggests that

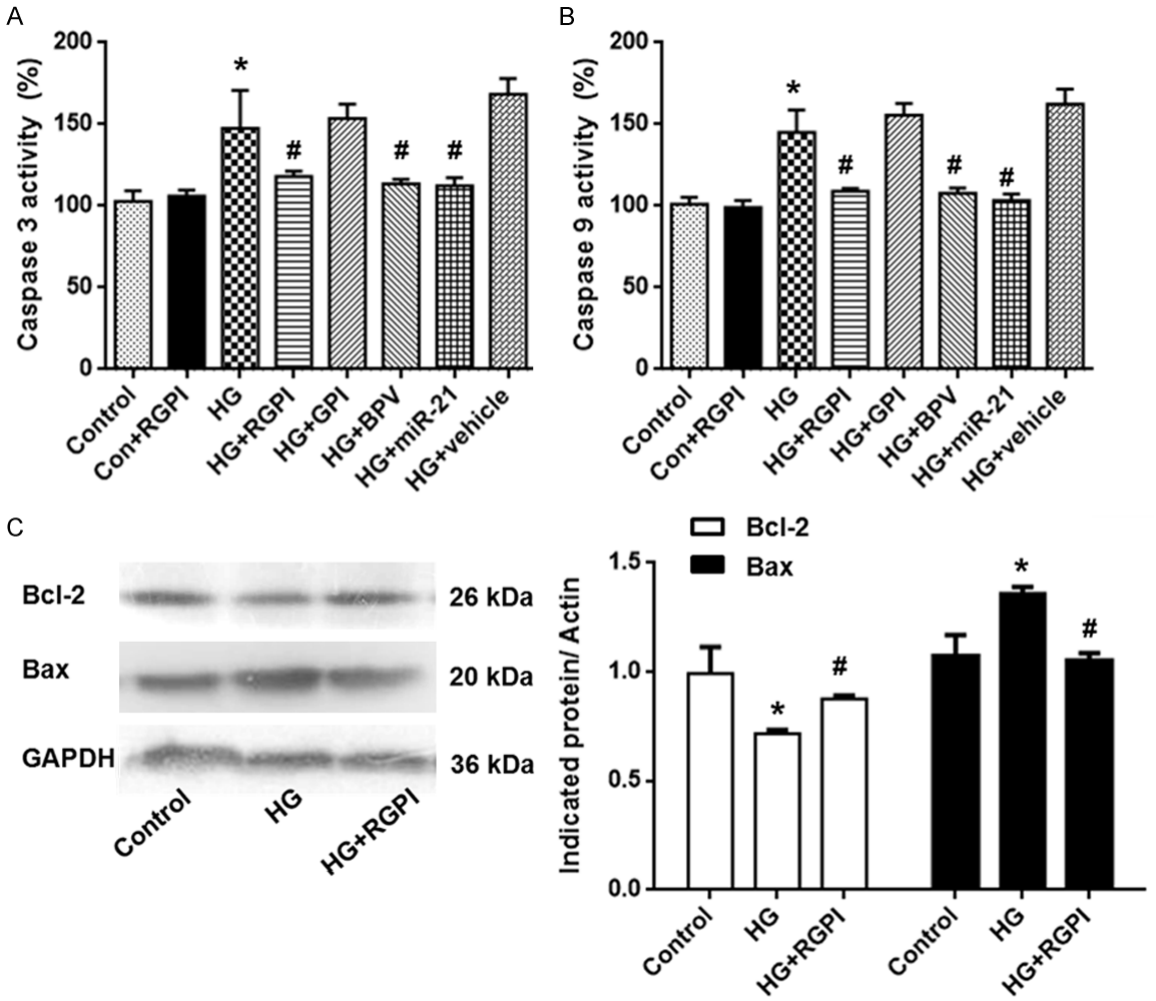

Figure 9. Reduced β2GPI prevents high glucose-induced apoptosis in HUVECs. The cells were incubated with reduced or non-reduced β2GPI for 48 h. After that, the cells were lysised and the activities of caspase 3, caspase 9 were tested. A. Caspase 3 activity; B. Caspase 9 activity; C. Expression of Bcl-2 and Bax. Data were presented as means and SEM. Six replications were carried out in each group. *P<0.05 compared with control; #P<0.05 compared with HG group.

PTEN displays critical functions in cell survival and death in the nervous system [39], and vascular system [8]. As previously reported, high glucose treatment can also promote PTEN expression [25], which attenuates the Akt signaling pathway. Akt is required for cell survival and the increase in Akt phosphorylation could explain the cell protection [33]. In the current study, it was observed that PTEN levels were promoted after a 48 h high glucose treatment. Additionally, a down-regulation of PTEN expression was found at a 6 h time point after high glucose treatment. These data might suggest that PTEN functions as a marker of environmental stress. In the acute phase, the down-regulation of PTEN might function to fight against adverse conditions. However, after a long-term treatment, PTEN was finally promoted to contribute to cell death. PTEN is the negative regulator of the Akt signaling pathway [40]. The current data also show that the dynamic changes in PTEN were inversely correlated with those of Akt phosphorylation. As predicted, high glucose initially promoted, but later decreased Akt phosphorylation. The inhibition of this signaling pathway would contribute to high glucose induced apoptosis [9, 41]. Additionally, the later decrease in p-Akt levels wasconsistent with previous findings [7].

In the current study, the phenomenon that high glucose caused a dynamic changein PTEN expression was demonstrated, and the results also established that miR-21 was responsible

for the PTEN dynamic change. Considering the well-established regulation of PTEN expression by miR-21, it was demonstrated that high glucose dynamically and inversely regulated miR-21 and PTEN. Moreover, it was shown that a miR-21 mimic could promote the high glucose induced increase in PTEN expression.

Additionally, it was shown that Rβ2GPI had a similar function as a miR-21 mimic. Rβ2GPI co-application not only promoted the high glucose-induced decrease in miR-21 expression, but also mitigated the increase in PTEN expression. However, Rβ2GPI alone did not affect miR-21 and PTEN expression in control HUVECs. These dataindicate that Rβ2GPI only reverses pathological, but not physiological alterations of miR-21. As predicted, Rβ2GPI did not affect Akt phosphorylation and cell viability in control HUVECs. In contrast, Rβ2GPI, a miR-21 mimic and a PTEN inhibitor exerted protection against high glucose-induced cell loss. Additionally, PTEN was genetically silenced to further confirm the protection it confers. Consistent with the data obtained using a PTEN inhibitor, PTEN silence also prevented high glucose-induced cell death. These results reveal that Rβ2GPI protects against high glucose induced cell loss via miR-21 and PTEN.

Calcium overloading is an important cause of cell death [42]. High glucose elicited calcium overloading in HUVECs, which was eliminated by Rβ2GPI. Interestingly, a miR-21 mimic, as well as PTEN inhibition, could mitigate the high glucose-induced increase in intracellular calcium. These data suggest that the calcium signaling pathway was located downstream of the death pathway. NO is an important neurotransmitter secreted by vascular endothelial cells. Many functions for NO, including inhibiting monocyte-macrophage and platelet adhesion, decreasing the monolayer permeability of vascular endothelial cells and reducing vascular endothelial cell and smooth muscle cell proliferation, have been found [43]. A total of 30% of the NO in the blood is derived from endothelial NOS genes expressed by vascular endothelial cells [44]. In the current study, increased NO levels and NOS activity were observed in high glucose-induced injury in HUVECs. The current data show that high glucose decreased NO levels and NOS activity and the abnormalities of NO genesis were prevented by Rβ2GPI treatment. Importantly, a miR-21 mimic, as well as a PTEN inhibitor, ameliorated NO production and NOS activity in high glucose-treated cells. Hyperglycemia-induced endothelial dysfunction could also be attributed to prostaglandin generation by COX. Interestingly, it was observed that high glucose treatment induced upregulation of COX-2, which is consistent with previous publications [45, 46]. An increase in COX-2 might lead to a decrease in NO and an altered prostanoid profile in human endothelial cells [45]. Critically, miR-21-regulated PTEN was also involved in the regulation of COX-2 activity.

Apoptosis is the major mechanism of cell death involved in high glucose-induced cell death [7]. Caspase-9 is an important downstream effector of mitochondria-dependent apoptosis. Cytochrome cis released from mitochondria after their impairment and the activation of caspase-9. Finally, caspase-9 activates caspase-3 to execute apoptosis. In the current study, caspase-9 and caspase-3 activities were assessed. It was found that high glucose promoted caspase-3 and caspase-9 activities. Moreover, Rβ2GPI reversed the increase in caspase 3 and caspase 9. Additionally, it was confirmed that Rβ2GPI prohibited apoptosis through increasing Bcl-2 and decreasing Bax expression.

The current study provides *in vitro* data supporting the hypothesis that Rβ2GPI, but not β2GPI, exerts protection in high glucose-induced cell death. Extensive β2GPI is secreted in pathological conditions [47] and elevated serum β2-GPI-low-density lipoprotein levels have been proposed as a serological hallmark of enhanced LDL oxidation *in vivo* and are closely associated with the presence of diabetic microvascular complications [21]. Therefore, reducing β2GPI could be a potential candidate for the treatment of diabetic microvascular complications. An appropriate method to reduce β2GPI might be effective to prohibit disease progression. However, the current study is limited to a cell culture study. How to promote the reduction of β2GPI *in vivo* is still acritical questionregarding its applicationin clinical trials. Regarding the mechanisms, the current study also did not establish how Rβ2GPI regulates miR-21 expression. Potential membrane receptors, including epidermal growth factor receptor, cytokine receptor and receptor tyrosine kinases might activate miR-21 down-

stream [48]. Considering the macromolecular structure of Rβ2GPI, the potential target of Rβ2GPI might be associated with these receptors. However, further clarification is necessary to clearlyidentify these mechanisms.

Conclusion

In the current study, *in vitro* data demonstrating the protection provided by Rβ2GPI in high glucose induced cell injury in HUVECs have been provided. High glucose causing dynamic changes in miR-21 and PTEN might be the critical reason forcell death, NO production and COX-2 activation.

Acknowledgements

The authors gratefully acknowledge the financial support from the National Natural Science Foundation of China (NO. 81300665).

Disclosure of conflict of interest

None.

Address correspondence to: Qiu-Mei Zhang, Key Laboratory of Hormones and Development (Ministry of Health), Tianjin Key Laboratory of Metabolic Diseases, Tianjin Metabolic Diseases Hospital & Tianjin Institute of Endocrinology, Tianjin Medical University, 300070 Tianjin, China. Tel: 86 22-23333206; Fax: 86 22-23528640; E-mail: qiumei_zhang1@sina.com

References

[1] Tocci G, Ferrucci A, Guida P, Avogaro A, Comaschi M, Corsini A, Cortese C, Giorda CB, Manzato E, Medea G, Mureddu GF, Riccardi G, Titta G, Ventriglia G, Zito GB, Volpe M and Committee ES. Impact of diabetes mellitus on the clinical management of global cardiovascular risk: analysis of the results of the evaluation of final feasible effect of control training and ultra sensitization (EFFECTUS) educational program. Clin Cardiol 2011; 34: 560-566.

[2] Cade WT. Diabetes-related microvascular and macrovascular diseases in the physical therapy setting. Phys Ther 2008; 88: 1322-1335.

[3] Ceriello A. Postprandial hyperglycemia and diabetes complications: is it time to treat? Diabetes 2005; 54: 1-7.

[4] Tsukada S, Masuda H, Jung SY, Yun J, Kang S, Kim DY, Park JH, Ji ST, Kwon SM and Asahara T. Impaired development and dysfunction of endothelial progenitor cells in type 2 diabetic mice. Diabetes Metab 2017; 43: 154-162.

[5] Ren Y, Tao S, Zheng S, Zhao M, Zhu Y, Yang J and Wu Y. Salvianolic acid B improves vascular endothelial function in diabetic rats with blood glucose fluctuations via suppression of endothelial cell apoptosis. Eur J Pharmacol 2016; 791: 308-315.

[6] Jia G, Durante W and Sowers JR. Endothelium-derived hyperpolarizing factors: a potential therapeutic target for vascular dysfunction in obesity and insulin resistance. Diabetes 2016; 65: 2118-2120.

[7] Ho FM, Lin WW, Chen BC, Chao CM, Yang CR, Lin LY, Lai CC, Liu SH and Liau CS. High glucose-induced apoptosis in human vascular endothelial cells is mediated through NF-kappaB and c-Jun NH2-terminal kinase pathway and prevented by PI3K/Akt/eNOS pathway. Cell Signal 2006; 18: 391-399.

[8] Li JY, Huang WQ, Tu RH, Zhong GQ, Luo BB and He Y. Resveratrol rescues hyperglycemia-induced endothelial dysfunction via activation of Akt. Acta Pharmacol Sin 2017; 38: 182-191.

[9] Liu X, Chen D, Wu Z, Li J, Li J, Zhao H and Liu T. Ghrelin inhibits high glucose-induced 16 HBE cells apoptosis by regulating Wnt/beta-catenin pathway. Biochem Biophys Res Commun 2016; 477: 902-907.

[10] Rioche M and Masseyeff R. Synthesis of plasma beta 2 glycoprotein I by human hepatoma cells in tissue culture. Biomedicine 1974; 21: 420-423.

[11] Rahgozar S. Revisiting beta 2 glycoprotein I, the major autoantigen in the antiphospholipid syndrome. Iran J Immunol 2012; 9: 73-85.

[12] Blank M and Shoenfeld Y. Beta-2-glycoprotein-I, infections, antiphospholipid syndrome and therapeutic considerations. Clin Immunol 2004; 112: 190-199.

[13] Schwarzenbacher R, Zeth K, Diederichs K, Gries A, Kostner GM, Laggner P and Prassl R. Crystal structure of human beta2-glycoprotein I: implications for phospholipid binding and the antiphospholipid syndrome. EMBO J 1999; 18: 6228-6239.

[14] Wang QQ, Zhou SJ, Meng ZX, Wang J, Chen R, Lv L, Li CJ, Yu DM and Yu P. Domain I-IV of beta2-glycoprotein I inhibits advanced glycation end product-induced angiogenesis by down-regulating vascular endothelial growth factor 2 signaling. Mol Med Rep 2015; 11: 2167-2172.

[15] de Groot PG and Meijers JC. beta(2) -Glycoprotein I: evolution, structure and function. J Thromb Haemost 2011; 9: 1275-1284.

[16] Petri M. Update on anti-phospholipid antibodies in SLE: the Hopkins' lupus cohort. Lupus 2010; 19: 419-423.

[17] Agar C, de Groot PG, Marquart JA and Meijers JC. Evolutionary conservation of the lipopolysaccharide binding site of beta(2)-glycoprotein I. Thromb Haemost 2011; 106: 1069-1075.
[18] Jankowski M, Vreys I, Wittevrongel C, Boon D, Vermylen J, Hoylaerts MF and Arnout J. Thrombogenicity of beta 2-glycoprotein I-dependent antiphospholipid antibodies in a photochemically induced thrombosis model in the hamster. Blood 2003; 101: 157-162.
[19] Ioannou Y, Zhang JY, Passam FH, Rahgozar S, Qi JC, Giannakopoulos B, Qi M, Yu P, Yu DM, Hogg PJ and Krilis SA. Naturally occurring free thiols within beta 2-glycoprotein I in vivo: nitrosylation, redox modification by endothelial cells, and regulation of oxidative stress-induced cell injury. Blood 2010; 116: 1961-1970.
[20] Wang C, Niu DM, Hu J, Guan XC, Yang W, Wang JJ, Zhang CY and Zhang CN. Elevated serum beta2-glycoprotein-I-lipoprotein(a) complexes levels are associated with the presence and complications in type 2 diabetes mellitus. Diabetes Res Clin Pract 2013; 100: 250-256.
[21] Yu R, Yuan Y, Niu D, Song J, Liu T, Wu J and Wang J. Elevated beta2-glycoprotein I-low-density lipoprotein levels are associated with the presence of diabetic microvascular complications. J Diabetes Complications 2015; 29: 59-63.
[22] Yu P, Passam FH, Yu DM, Denyer G and Krilis SA. Beta2-glycoprotein I inhibits vascular endothelial growth factor and basic fibroblast growth factor induced angiogenesis through its amino terminal domain. J Thromb Haemost 2008; 6: 1215-1223.
[23] Ma J, Zhang JY, Liu Y, Yu DM and Yu P. Redox status of beta 2 GPI in different stages of diabetic angiopathy. Dis Markers 2016; 2016: 8246839.
[24] Rahdar M, Inoue T, Meyer T, Zhang J, Vazquez F and Devreotes PN. A phosphorylation-dependent intramolecular interaction regulates the membrane association and activity of the tumor suppressor PTEN. Proc Natl Acad Sci U S A 2009; 106: 480-485.
[25] Lv Q, Xue Y, Li G, Zou L, Zhang X, Ying M, Wang S, Guo L, Gao Y, Li G, Xu H, Liu S, Xie J and Liang S. Beneficial effects of evodiamine on P2X(4)-mediated inflammatory injury of human umbilical vein endothelial cells due to high glucose. Int Immunopharmacol 2015; 28: 1044-1049.
[26] Lin KY, Wang HH, Lai ST, Pan JP and Chiang AN. beta (2)-glycoprotein I protects J774A.1 macrophages and human coronary artery smooth muscle cells against apoptosis. J Cell Biochem 2005; 94: 485-496.
[27] Zhang R, Zhou SJ, Li CJ, Wang XN, Tang YZ, Chen R, Lv L, Zhao Q, Xing QL, Yu DM and Yu P. C-reactive protein/oxidised low-density lipoprotein/beta 2-glycoprotein I complex promotes atherosclerosis in diabetic BALB/c mice via p38mitogen-activated protein kinase signal pathway. Lipids Health Dis 2013; 12: 42.
[28] Wang T, Chen SS, Chen R, Yu DM and Yu P. Reduced beta 2 glycoprotein I improves diabetic nephropathy via inhibiting TGF-beta1-p38 MAPK pathway. Int J Clin Exp Pathol 2015; 8: 2321-2333.
[29] Passam FH, Rahgozar S, Qi M, Raftery MJ, Wong JW, Tanaka K, Ioannou Y, Zhang JY, Gemmell R, Qi JC, Giannakopoulos B, Hughes WE, Hogg PJ and Krilis SA. Redox control of beta 2-glycoprotein I-von Willebrand factor interaction by thioredoxin-1. J Thromb Haemost 2010; 8: 1754-1762.
[30] Deevi R, Fatehullah A, Jagan I, Nagaraju M, Bingham V and Campbell FC. PTEN regulates colorectal epithelial apoptosis through Cdc42 signalling. Br J Cancer 2011; 105: 1313-1321.
[31] Xue L, Xu F, Meng L, Wei S, Wang J, Hao P, Bian Y, Zhang Y and Chen Y. Acetylation-dependent regulation of mitochondrial ALDH2 activation by SIRT3 mediates acute ethanol-induced eNOS activation. FEBS Lett 2012; 586: 137-142.
[32] Zhu G, Li J, He L, Wang X and Hong X. MPTP-induced changes in hippocampal synaptic plasticity and memory are prevented by memantine through the BDNF-TrkB pathway. Br J Pharmacol 2015; 172: 2354-2368.
[33] Zhu G, Wang X, Wu S and Li Q. Involvement of activation of PI3K/Akt pathway in the protective effects of puerarin against MPP+-induced human neuroblastoma SH-SY5Y cell death. Neurochem Int 2012; 60: 400-408.
[34] Shi B, Deng W, Long X and Wang Y. TCT-823 miR-21 reduces hydrogen peroxide-induced apoptosis in c-kit+ cardiac stem cells in vitro through PTEN/PI3K/Akt signaling. J Am Coll Cardiol 2016; 68: B333.
[35] Stambolic V, Suzuki A, de la Pompa JL, Brothers GM, Mirtsos C, Sasaki T, Ruland J, Penninger JM, Siderovski DP and Mak TW. Negative regulation of PKB/Akt-dependent cell survival by the tumor suppressor PTEN. Cell 1998; 95: 29-39.
[36] Xu Q, Wink DA and Colton CA. Nitric oxide production and regulation of neuronal NOS in tyrosine hydroxylase containing neurons. Exp Neurol 2004; 188: 341-350.
[37] Blank M, Baraam L, Eisenstein M, Fridkin M, Dardik R, Heldman Y, Katchalski-Katzir E and Shoenfeld Y. beta 2-Glycoprotein-I based peptide regulate endothelial-cells tissue-factor expression via negative regulation of pGSK3

beta expression and reduces experimental-antiphospholipid-syndrome. J Autoimmun 2011; 37: 8-17.

[38] Rand JH, Wu XX, Quinn AS, Chen PP, Hathcock JJ and Taatjes DJ. Hydroxychloroquine directly reduces the binding of antiphospholipid antibody-beta 2-glycoprotein I complexes to phospholipid bilayers. Blood 2008; 112: 1687-1695.

[39] Chen X, Du YM, Xu F, Liu D and Wang YL. Propofol prevents hippocampal neuronal loss and memory impairment in cerebral ischemia injury through promoting PTEN degradation. J Mol Neurosci 2016; 60: 63-70.

[40] Tachibana N, Cantrup R, Dixit R, Touahri Y, Kaushik G, Zinyk D, Daftarian N, Biernaskie J, McFarlane S and Schuurmans C. Pten regulates retinal amacrine cell number by modulating akt, tgfbeta, and erk signaling. J Neurosci 2016; 36: 9454-9471.

[41] Liu Y, Tian X, Li Y, Liu D, Liu M, Zhang X, Zhang Q, Yan C and Han Y. Up-regulation of CREG expression by the transcription factor GATA1 inhibits high glucose- and high palmitate-induced apoptosis in human umbilical vein endothelial cells. PLoS One 2016; 11: e0154861.

[42] Choi SE, Min SH, Shin HC, Kim HE, Jung MW and Kang Y. Involvement of calcium-mediated apoptotic signals in H_2O_2-induced MIN6N8a cell death. Eur J Pharmacol 2006; 547: 1-9.

[43] Botham KM and Wheeler-Jones CP. Postprandial lipoproteins and the molecular regulation of vascular homeostasis. Prog Lipid Res 2013; 52: 446-464.

[44] McCullagh KJ, Cooney R and O'Brien T. Endothelial nitric oxide synthase induces heat shock protein HSPA6 (HSP70B') in human arterial smooth muscle cells. Nitric Oxide 2016; 52: 41-48.

[45] Sheu ML, Ho FM, Yang RS, Chao KF, Lin WW, Lin-Shiau SY and Liu SH. High glucose induces human endothelial cell apoptosis through a phosphoinositide 3-kinase-regulated cyclooxygenase-2 pathway. Arterioscler Thromb Vasc Biol 2005; 25: 539-545.

[46] Chen JH, Hsiao G, Lee AR, Wu CC and Yen MH. Andrographolide suppresses endothelial cell apoptosis via activation of phosphatidyl inositol-3-kinase/Akt pathway. Biochem Pharmacol 2004; 67: 1337-1345.

[47] Zhang Q, Zhu L, Zheng M, Fan C, Li Y, Zhang D, He Y and Yang H. Changes of serum omentin-1 levels in normal subjects, type 2 diabetes and type 2 diabetes with overweight and obesity in Chinese adults. Ann Endocrinol (Paris) 2014; 75: 171-175.

[48] Venturutti L, Romero LV, Urtreger AJ, Chervo MF, Cordo Russo RI, Mercogliano MF, Inurrigarro G, Pereyra MG, Proietti CJ, Izzo F, Diaz Flaque MC, Sundblad V, Roa JC, Guzman P, Bal de Kier Joffe ED, Charreau EH, Schillaci R and Elizalde PV. Stat 3 regulates ErbB-2 expression and co-opts ErbB-2 nuclear function to induce miR-21 expression, PDCD4 downregulation and breast cancer metastasis. Oncogene 2016; 35: 2208-2222.